

Kinetics of indirect excitons in an optically induced trap in GaAs quantum wells

A. T. Hammack,¹ L. V. Butov,¹ L. Mouchliadis,² A. L. Ivanov,² and A. C. Gossard³¹*Department of Physics, University of California at San Diego, La Jolla, California 92093-0319, USA*²*Department of Physics and Astronomy, Cardiff University, Cardiff CF24 3AA, United Kingdom*³*Materials Department, University of California at Santa Barbara, Santa Barbara, California 93106-5050, USA*

(Received 12 September 2007; published 16 November 2007)

We report on the kinetics of a low-temperature gas of indirect excitons in an optically induced exciton trap. The excitons in the region of laser excitation are found to rapidly—within 4 ns—cool to the lattice temperature $T=1.4$ K, while the excitons at the trap center are found to be cold—essentially at the lattice temperature—even during the excitation pulse. The loading time of excitons to the trap center is about 40 ns, longer than the cooling time yet shorter than the lifetime of the indirect excitons. The observed time hierarchy is favorable for creating a dense and cold exciton gas in optically induced traps and for *in situ* control of the gas by varying the excitation profile in space and time before the excitons recombine.

DOI: [10.1103/PhysRevB.76.193308](https://doi.org/10.1103/PhysRevB.76.193308)

PACS number(s): 78.67.De, 05.30.Jp, 73.63.Hs

The modern advent of optical and magnetic trapping of atomic gases^{1–4} has led to the observation of new states of matter such as Bose-Einstein condensates in atomic gases^{5,6} and atomic degenerate Fermi gases.⁷ Optical trapping allowed the creation of a variety of potential reliefs for atoms, including optical lattices,^{8,9} and control of these reliefs *in situ*. One of the most important characteristics, which is crucial for the observation, probe, and control of these new states, is the trap loading time. Apparently, studies of the degenerate gases in the traps require the fast loading of the gases to the trap, preferably on a time scale less than their lifetime in the trap. For the typical optical traps, the loading times of the degenerate atomic gases are on the order of a few tens of seconds, while their lifetimes in the trap are on the order of a few seconds.^{10,11}

The system of excitons offers an opportunity to study degenerate Bose gases in trap potentials in semiconductor materials. Their low mass results in a high temperature of quantum degeneracy for excitons T_{dB} on the order of 1 K.¹² For instance, for excitons in a quantum well $T_{\text{dB}} = 2\pi\hbar^2 n_{2\text{D}} / (mgk_{\text{B}}) \approx 3$ K at the exciton density per spin state $n_{2\text{D}}/g = 10^{10}$ cm⁻². Exciton gases with temperatures well below 1 K and densities higher than 10^{10} cm⁻² can be realized in coupled quantum well (CQW) structures.¹³ The indirect excitons in CQWs can cool down to these low temperatures due to their long lifetimes and high cooling rates.¹⁴

Indirect excitons in CQWs can be confined by a variety of trapping potentials including strain-induced traps,^{15–17} traps created by laser-induced interdiffusion,¹⁸ electrostatic traps,^{19–22} magnetic traps,²³ and optically induced traps.²⁴ Two of these trap types—the electrostatic and optically induced traps—show promise of rapid and effective control of the excitons by varying in space and time the gate voltage pattern and the laser intensity pattern, respectively. Control of excitons by varying the electrostatic potential on a time scale much shorter than the exciton lifetime was recently demonstrated.²⁵ This indicates the feasibility of studying excitons in controlled electrostatic traps. However, the time scale of exciton control in an optically induced trap remained unknown before this work.

In this Brief Report, we present studies of the spatial and spectral kinetics of excitons in an optically induced trap. The results demonstrate a rapid loading of the trap by cold excitons on a time scale less than the exciton lifetime and prove the feasibility of accumulating a spatially confined dense and cold exciton gas as well as the rapid *in situ* control of excitons in the traps.

The experimental measurements were performed using time-resolved imaging with 4 ns time resolution and 2 μm spatial resolution. The excitons were photogenerated using rectangular laser excitation pulses emitted by a pulsed semiconductor laser diode at 635 nm. The pulse duration was 500 ns, the edge sharpness <1 ns, and the repetition frequency 1 MHz. The period and duty cycle were chosen to provide ample time for the exciton gas to reach equilibrium during the laser pulse and to allow complete decay of the indirect exciton photoluminescence (PL) between the pulses. The pulses were patterned into a laser excitation ring with a diameter of 30 μm and a ring thickness following a Gaussian profile of full width at half maximum $=2\sigma \approx 10$ μm using a shadow mask. This ring-shaped laser excitation created the in-plane spatial confinement of cold indirect excitons by exploiting their mean-field repulsive interaction, which forms the trapping profile.²⁴ Time-dependent spatial x - y and spectral E - y PL images were acquired by a nitrogen-cooled charge coupled device (CCD) camera after passing through a time-gated PicoStar HR TauTec intensifier with a time-integration window of 4 ns. For x - y imaging, an interference filter, chosen to match the indirect exciton energy exclusively, is placed in the optical path before the time-gated intensifier. In this manner, both the high intensity low-energy bulk emission and direct exciton emission are removed. The spectral filtering and time-gated imaging combine to allow the direct visualization of the intensity profile of the indirect exciton emission in spatial coordinates as a function of delay time τ [see Figs. 1(a)–1(d)]. The time-dependent measurements of the indirect exciton spectra were acquired by placing the time-gated intensifier and CCD after a single grating spectrometer.

The CQW structure used in these experiments was grown by molecular beam epitaxy and contains two 8 nm GaAs QWs separated by a 4 nm Al_{0.33}Ga_{0.67}As barrier (details on

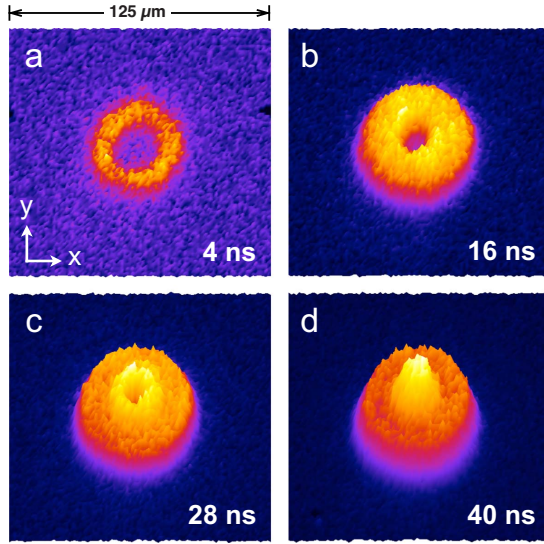


FIG. 1. (Color online) Time-resolved images of laser-induced trapping of excitons collected by a photogated CCD. [(a)–(d)] x - y plots of the PL intensity from indirect excitons collected at delays of 4, 16, 28, and 40 ns relative to the start of 635 nm pulsed laser diode excitation in a 30 μm diameter ring on the CQW sample. The time-integration window for each image is 4 ns. Average excitation power $P_{\text{ex}}=75 \mu\text{W}$. Bath temperature $T_b=1.4 \text{ K}$. $V_g=1.2 \text{ V}$.

the CQW structures can be found in Ref. 13). Indirect excitons in the CQW structure are formed from electrons and holes confined to different QWs. Separation between the electron and hole layers in the CQW structure causes the optical lifetime τ_{opt} of the indirect excitons to exceed that of regular direct excitons by orders of magnitude and is $\tau_{\text{opt}} \approx 50 \text{ ns}$ at $V_g=1.2 \text{ V}$ for the studied CQW sample. The exciton density profile was estimated from the measured exciton energy profiles in E - y coordinates using the relation between the energy and density of the indirect excitons $\delta E = u_0 n_{2\text{D}}$, where $u_0=4\pi e^2 d/\epsilon_b$.^{26–29} For the studied CQW sample, $\epsilon_b=12.9$ and $d=11.5 \text{ nm}$.¹³

The kinetics presented in Figs. 2(c) and 2(d) demonstrate that the exciton pattern reaches a stationary state and, therefore, the trap loading is completed within about 40 ns. Thus, the trap loading time is about the lifetime of indirect excitons in this CQW sample [see Fig. 3(c)]. Note that in another CQW sample with a larger separation between the electron and hole layers, the lifetime of indirect excitons reaches several microseconds,²⁵ which is much larger than the trap loading time reported here. However, trap loading on a time scale comparable to the lifetime in the trap is already favorable for studies of confined degenerate gases.^{10,11}

Furthermore, for the excitation power used in the experiments, the density of excitons at the trap center reaches $n_{2\text{D}} \approx 1.4 \times 10^{10} \text{ cm}^{-2}$ within 40 ns. As shown below, the exciton gas is cold, essentially at the lattice temperature, within the area $\sim 100 \mu\text{m}^2$ around the trap center. Therefore, $\sim 10^4$ cold excitons are loaded to the trap over the course of 40 ns. The corresponding collection rate of cold excitons to the optically induced exciton trap exceeds 10^{11} excitons/s.

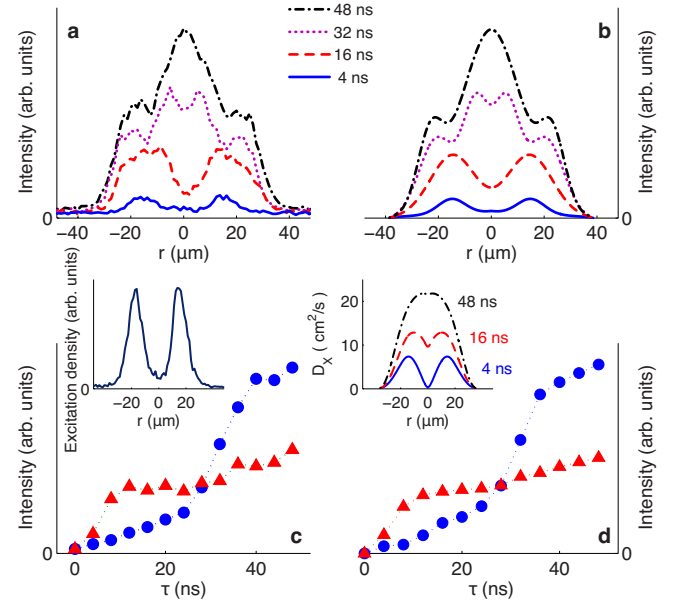


FIG. 2. (Color online) Kinetics of the indirect exciton PL profile following the onset of the ring-shaped laser excitation pulse. The (a) measured and (b) calculated cross sections of the indirect exciton PL across the diameter of the laser excitation ring as a function of time. The (c) measured and (d) calculated indirect exciton PL intensities at the ring center (blue/dark gray circles) and in the area of the laser excitation ring (red/light gray triangles) as a function of time. The time-integration window for each [(a) and (b)] profile and [(c) and (d)] point is 4 ns. $\tau=0$ and $\tau=500 \text{ ns}$ correspond to the onset and termination of the rectangular laser excitation pulse, respectively. Left inset: the ring-shaped laser excitation profile. Right inset: the calculated radial dependence of the exciton diffusion coefficient for different time delays. Average excitation power $P_{\text{ex}}=75 \mu\text{W}$. Bath temperature $T_b=1.4 \text{ K}$. $V_g=1.2 \text{ V}$.

In order to model the experimental data, we use the coupled drift-diffusion and thermalization equations for the exciton effective temperature T and density $n_{2\text{D}}$

$$\frac{\partial n_{2\text{D}}}{\partial t} = \nabla [D_x \nabla n_{2\text{D}} + \mu_x n_{2\text{D}} \nabla (u_0 n_{2\text{D}})] - \frac{n_{2\text{D}}}{\tau_{\text{opt}}} + \Lambda, \quad (1)$$

$$\frac{\partial T}{\partial t} = \left(\frac{\partial T}{\partial t} \right)_{n_{2\text{D}}} + S_{\text{pump}} + S_{\text{opt}}, \quad (2)$$

where D_x , μ_x , $\tau_{\text{opt}}=\tau_{\text{opt}}(n_{2\text{D}}, T)$, and $\Lambda=\Lambda(r_{\parallel}, t)$ are the diffusion coefficient, mobility, optical lifetime, and generation rate of indirect excitons, respectively.^{29,30} The term $(\partial T/\partial t)_{n_{2\text{D}}}$ describes cooling of indirect excitons due to their coupling with bulk LA phonons,³¹ and the terms S_{pump} and S_{opt} refer to heating of indirect excitons by the laser field and recombination heating or cooling of the particles, as detailed in Ref. 30. The stationary solution of these equations for laser-induced traps is discussed in Ref. 30. In the present work, Eqs. (1) and (2) are analyzed to model the trapping kinetics, i.e., in the space and time domain.

The effective $n_{2\text{D}}$ -dependent screening of the disorder potential $U_{\text{rand}}(r_{\parallel})$ by dipole-dipole interacting indirect excitons

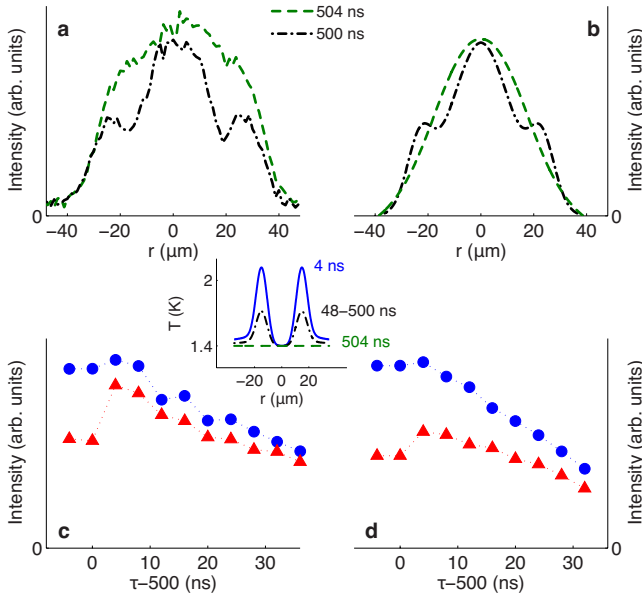


FIG. 3. (Color online) Indirect exciton PL following the termination of the ring-shaped laser excitation pulse. The (a) measured and (b) calculated cross sections of the indirect exciton PL across the diameter of the laser excitation ring as a function of time. The (c) measured and (d) calculated indirect exciton PL intensities at the ring center (blue/dark gray circles) and in the area of the laser excitation ring (red/light gray triangles) as a function of time. The time-integration window for each [(a) and (b)] profile and [(c) and (d)] point is 4 ns. $\tau=0$ and $\tau=500$ ns correspond to the onset and termination of the rectangular laser excitation pulse, respectively. Inset: the calculated temperature across the ring diameter in the beginning of the laser excitation pulse at $\tau=4$ ns (blue/dark gray), in the stationary regime achieved during the 500-ns-long excitation pulse about 40 ns after its start at $\tau=48-500$ ns (black), and 4 ns after the termination of the laser excitation pulse at $\tau=504$ ns (green/light gray). Average excitation power $P_{\text{ex}}=75 \mu\text{W}$. Bath temperature $T_b=1.4$ K. $V_g=1.2$ V.

is crucial for the drastic decrease of the time needed to fill up the optically induced trap with indirect excitons. The thermionic model, derived from Eq. (1) for a long-range correlated disorder potential, yields the effective diffusion coefficient,

$$D_x = D_x^{(0)} \exp\left[-\frac{U^{(0)}}{k_B T + u_0 n_{2D}}\right], \quad (3)$$

where $U^{(0)}=2(|\langle U_{\text{rand}}(\mathbf{r}_{\parallel}) \rangle - \langle U_{\text{rand}}(\mathbf{r}_{\perp}) \rangle|)$ and $D_x^{(0)}$ is the in-plane diffusion coefficient in the absence of CQW disorder.²⁹

By using Eq. (3), the time τ_{trav} required for an indirect exciton to travel from the boundary of an annular trap of radius R to its center is estimated as

$$\tau_{\text{trav}}^{(1)} = \frac{R^2}{D_x^{(0)}} e^{U^{(0)}/k_B T} \quad \text{for } k_B T \gg u_0 n_{2D}, \quad (4)$$

$$\tau_{\text{trav}}^{(2)} = \frac{R^2}{D_x^{(0)}} \frac{k_B T}{u_0 n_{2D}^{(0)}} e^{U^{(0)}/(u_0 n_{2D}^{(0)})} \quad \text{for } k_B T \ll u_0 n_{2D}, \quad (5)$$

where $n_{2D}^{(0)}$ is the density of photoexcited indirect excitons at the boundary of the trap, and the first, low-density limit

($n_{2D} < 10^9 \text{ cm}^{-2}$) refers to the unscreened disorder potential, while the second, high-density limit ($n_{2D} \geq 10^{10} \text{ cm}^{-2}$) deals with effective mean-field screening of $U_{\text{rand}}(\mathbf{r}_{\parallel})$. In the low-density limit, the excitons are essentially localized by disorder, the diffusion coefficient is small, $D_x = D_x^{(0)} \times \exp[-U^{(0)}/(k_B T)] \sim 0.1 \text{ cm}^2/\text{s}$, and the in-plane transport of excitons out of the excitation spot cannot be seen because, in this case, $\tau_{\text{trav}}^{(1)} \gg \tau_{\text{opt}}$. In contrast, for $k_B T \ll u_0 n_{2D}$, the diffusion coefficient is large, $D_x = D_x^{(0)} \exp[-U^{(0)}/(u_0 n_{2D})] \sim 10 \text{ cm}^2/\text{s}$, giving rise to the drastic decrease of the characteristic travel time τ_{trav} : According to Eqs. (4) and (5), $\tau_{\text{trav}}^{(2)} = \beta \tau_{\text{trav}}^{(1)} \ll \tau_{\text{trav}}^{(1)}$ with the dimensionless smallness parameter $\beta \sim 10^{-3} - 10^{-5}$ (for $T \sim 1\text{K}$, $U_0 \sim 1 \text{ meV}$, and $n_{2D} \sim 10^{10} \text{ cm}^{-2}$). The transition from localized to delocalized indirect excitons is indeed observed with increasing density.^{24,30,32}

The calculated change of the exciton diffusion coefficient, due to screening of CQW disorder, is shown in the right inset of Fig. 2. A drastic increase of D_x with increasing n_{2D} is consistent with the above estimates. For our experiments, evaluations with Eq. (5) yield $\tau_{\text{trav}}^{(2)} \approx 4.6$ ns against $\tau_{\text{opt}} \approx 50$ ns; i.e., the condition $\tau_{\text{trav}}^{(2)} \ll \tau_{\text{opt}}$ is clearly met.

The numerical simulations were done by using control parameters consistent with those found in our previous studies^{14,24} of similar structures: $u_0 = 1.6 \times 10^{-10} \text{ meV cm}^2$, $U^{(0)} = 1.2 \text{ meV}$, $D_x^{(0)} = 35 \text{ cm}^2/\text{s}$, $m = 0.215 m_0$ (m_0 is the free electron mass), $E_x = 1.55 \text{ eV}$, and the deformation potential of exciton—LA-phonon interaction $D_{\text{DP}} = 6.5 \text{ eV}$. As can be seen in Figs. 2 and 3, the measured and calculated kinetics of the exciton spatial patterns are in quantitative agreement.

When the laser pulse is switched off, a jump in the exciton PL is observed in the region of laser excitation (Fig. 3). As shown in previous studies,³³ only low-energy excitons with the kinetic energy from the radiative zone, $E < E_0 \approx E_x \epsilon_b / (2mc^2)$, are optically active. The PL jump is caused by the increase of the radiative zone population due to the cooling of high-energy optically dark excitons after abruptly switching off the laser excitation.¹⁴ The time-resolved imaging experiments show that the PL jump is observed only in the region of laser excitation, where indirect excitons are effectively heated by the laser field. In this region, after switching off the laser excitation (Fig. 3), the excitons rapidly cool down to the lattice temperature $T_b = 1.4$ K within 4 ns, the time resolution of the current experiments. The calculated cooling (i.e., thermalization) time is $\tau_{\text{th}} \approx 0.2$ ns. Both the experiment and calculations show that the exciton cooling time to the lattice temperature is much shorter than the exciton lifetime $\tau_{\text{opt}} \approx 50$ ns.

More importantly, the data show no PL jump at the trap center (Fig. 3). This proves that the excitons at the trap center are cold, essentially at the lattice temperature T_b , even in the presence of the excitation pulse. The numerical simulations of the exciton temperature profile, $T = T(r_{\parallel})$, plotted in the inset of Fig. 3 for various time delays, are consistent with this observation. The hierarchy of times, $\tau_{\text{th}} \ll \tau_{\text{trav}} \ll \tau_{\text{opt}}$, results in complete thermalization of indirect excitons during their travel from the boundary of the optically induced trap to its center, where heating from the laser excitation is negligible.

In conclusion, we have found that the characteristic loading time of an optically induced trap with cold excitons is on the scale of tens of nanoseconds. The observed hierarchy of times (exciton cooling time) $<$ (trap loading time) $<$ (exciton lifetime in the trap) is favorable for creating a dense and cold exciton gas in the

optically induced traps and its *in situ* control by varying the excitation profile in space and time before the exciton recombination.

This work was supported by ARO under Grant No. W911NF-05-1-0527 and NSF under Grant No. DMR-0606543.

-
- ¹S. Chu, Rev. Mod. Phys. **70**, 685 (1998).
²C. N. Cohen-Tannoudji, Rev. Mod. Phys. **70**, 707 (1998).
³W. D. Phillips, Rev. Mod. Phys. **70**, 721 (1998).
⁴A. Ashkin, IEEE J. Sel. Top. Quantum Electron. **6**, 841 (2000).
⁵E. A. Cornell and C. E. Wieman, Rev. Mod. Phys. **74**, 875 (2002).
⁶W. Ketterle, Rev. Mod. Phys. **74**, 1131 (2002).
⁷B. DeMarco and D. S. Jin, Science **285**, 1703 (1999).
⁸M. Greiner, O. Mandel, T. Esslinger, T. W. Hänsch, and I. Bloch, Nature (London) **415**, 39 (2002).
⁹J. K. Chin, D. E. Miller, Y. Liu, C. Stan, W. Setiawan, C. Sanner, K. Xu, and W. Ketterle, Nature (London) **443**, 961 (2006).
¹⁰H. J. Lewandowski, D. M. Harber, D. L. Whitaker, and E. A. Cornell, J. Low Temp. Phys. **132**, 309 (2003).
¹¹E. W. Streed, A. P. Chikkatur, T. L. Gustavson, M. Boyd, T. Torii, D. Schneble, G. K. Campbell, D. E. Pritchard, and W. Ketterle, Rev. Sci. Instrum. **77**, 023106 (2006).
¹²L. V. Keldysh and A. N. Kozlov, Zh. Eksp. Teor. Fiz. **54**, 978 (1968) [Sov. Phys. JETP **27**, 521 (1968)].
¹³L. V. Butov, J. Phys.: Condens. Matter **16**, R1577 (2004).
¹⁴L. V. Butov, A. L. Ivanov, A. Imamoglu, P. B. Littlewood, A. A. Shashkin, V. T. Dolgoplov, K. L. Campman, and A. C. Gossard, Phys. Rev. Lett. **86**, 5608 (2001).
¹⁵J. P. Wolfe, W. L. Hansen, E. E. Haller, R. S. Markiewicz, C. Kittel, and C. D. Jeffries, Phys. Rev. Lett. **34**, 1292 (1975).
¹⁶D. P. Trauernicht, A. Mysyrowicz, and J. P. Wolfe, Phys. Rev. B **28**, 3590 (1983).
¹⁷K. Kash, J. M. Worlock, M. D. Sturge, P. Grabbe, J. P. Harbison, A. Scherer, and P. S. D. Lin, Appl. Phys. Lett. **53**, 782 (1988).
¹⁸K. Brunner, U. Bockelmann, G. Abstreiter, M. Walther, G. Böhm, G. Tränkle, and G. Weimann, Phys. Rev. Lett. **69**, 3216 (1992).
¹⁹S. Zimmermann, A. O. Govorov, W. Hansen, J. P. Kotthaus, M. Bichler, and W. Wegscheider, Phys. Rev. B **56**, 13414 (1997).
²⁰T. Huber, A. Zrenner, W. Wegscheider, and M. Bichler, Phys. Status Solidi A **166**, R5 (1998).
²¹A. T. Hammack, N. A. Gippius, S. Yang, G. O. Andreev, L. V. Butov, M. Hanson, and A. C. Gossard, J. Appl. Phys. **99**, 066104 (2006).
²²G. Chen, R. Rapaport, L. N. Pfeifer, K. West, P. M. Platzman, S. Simon, Z. Vörös, and D. Snoke, Phys. Rev. B **74**, 045309 (2006).
²³P. C. M. Christianen, F. Piazza, J. G. S. Lok, J. C. Maan, and W. van der Vleuten, Physica B **249**, 624 (1998).
²⁴A. T. Hammack, M. Griswold, L. V. Butov, L. E. Smallwood, A. L. Ivanov, and A. C. Gossard, Phys. Rev. Lett. **96**, 227402 (2006).
²⁵A. G. Winbow, A. T. Hammack, L. V. Butov, and A. C. Gossard, Nano Lett. **7**, 1349 (2007).
²⁶D. Yoshioka and A. H. MacDonald, J. Phys. Soc. Jpn. **59**, 4211 (1990).
²⁷X. Zhu, P. B. Littlewood, M. Hybertsen, and T. Rice, Phys. Rev. Lett. **74**, 1633 (1995).
²⁸S. B. de-Leon and B. Laikhtman, Phys. Rev. B **63**, 125306 (2001).
²⁹A. L. Ivanov, Europhys. Lett. **59**, 586 (2002).
³⁰A. L. Ivanov, L. E. Smallwood, A. T. Hammack, S. Yang, L. V. Butov, and A. C. Gossard, Europhys. Lett. **73**, 920 (2006).
³¹A. L. Ivanov, P. B. Littlewood, and H. Haug, Phys. Rev. B **59**, 5032 (1999).
³²L. V. Butov, A. C. Gossard, and D. S. Chemla, Nature (London) **418**, 751 (2002).
³³J. Feldmann, G. Peter, E. O. Gobel, P. Dawson, K. Moore, C. Foxon, and R. J. Elliott, Phys. Rev. Lett. **59**, 2337 (1987).